Original Article

FTO-mediated m^{6}A demethylation of SERPINE1 mRNA promotes tumor progression in hypopharyngeal squamous cell carcinoma

Na Sa[1#], Xuliang Liu[1#], Dake Hao[2,3], Zhenghua Lv[1], Shengli Zhou[1], Linxue Yang[1], Shan Jiang[1], Jiajun Tian[1], Wei Xu[1]

[1]Department of Otolaryngology-Head and Neck Surgery, Shandong Provincial ENT Hospital, Shandong University, Jinan, China; [2]Department of Surgery, School of Medicine, University of California Davis, Sacramento, CA, USA; [3]Institute for Pediatric Regenerative Medicine, Shriners Hospitals for Children, Sacramento, CA, USA

Contributions: (I) Conception and design: W Xu, J Tian; (II) Administrative support: N Sa, X Liu, W Xu; (III) Provision of study materials or patients: Z Lv, W Xu; (IV) Collection and assembly of data: S Zhou, S Jiang; (V) Data analysis and interpretation: D Hao, L Yang; (VI) Manuscript writing: All authors; (VII) Final approval of manuscript: All authors.

[#]These authors contributed equally to this work.

Correspondence to: Wei Xu, PhD; Jiajun Tian, PhD. Department of Otolaryngology-Head and Neck Surgery, Shandong Provincial ENT Hospital, Shandong University, No. 4, Duanxing West Road, Huaiyin District, Jinan 250012, China. Email: xuwhns@126.com; tianjiajun212@163.com.

Background: The fat mass and obesity-associated protein (FTO) is implicated in various diseases and acts as a demethylase for the most abundant modification of mRNA, namely N6-methyladenosine (m^{6}A) modification. It is known that FTO may play an oncogenic role or a tumor-suppressor role in different malignancies. The aim of this study was to investigate the functional roles of FTO in regulating biological processes related to hypopharyngeal squamous cell carcinoma (HSCC).

Methods: Using immunohistochemistry, quantitative real-time polymerase chain reaction (RT-qPCR), and Western blot analysis, we compared the expression levels of FTO in HSCC tissues to adjacent non-cancerous tissues. Furthermore, we evaluated the prognosis of patients with hypopharyngeal cancer in relation to FTO expression levels. *In vitro*, the Cell Counting Kit-8 (CCK8), wound healing assay, migration and invasion assays were used to identify roles of FTO in HSCC cells FaDu. Tumor xenografts in nude mice were used to disclose the effect of FTO *in vivo*. Then, transcriptome RNA sequencing (RNA-seq) assays were applied to screen for possible target genes. To confirm the specific site for modulating the expression of the target gene, we used the SRAMP database and methylated RNA immunoprecipitation PCR (MeRIP-PCR).

Results: The results showed that FTO was highly expressed in hypopharyngeal cancer tissues and was correlated with clinicopathology of patients. FTO promoted the proliferation, invasion and migration of hypopharyngeal cancer cells *in vitro* through its demethylase action. *In vivo* experiments showed that FTO promoted the growth of subcutaneously implanted tumors of hypopharyngeal cancer cells and their metastasis. Moreover, we revealed that FTO affected the malignant biological behavior of hypopharyngeal cancer cells by regulating the m^{6}A modification level of SERPINE1 mRNA. FTO promoted epithelial-mesenchymal transformation (EMT) of hypopharyngeal cancer cells through the SERPINE1 signaling axis.

Conclusions: Our study highlighted the functional significance of the FTO/SERPINE1 axis in tumorigenesis of HSCC. Targeting FTO holds promise as a new therapeutic strategy for HSCC.

Keywords: Hypopharyngeal squamous cell carcinoma (HSCC); fat mass and obesity-associated protein (FTO); SERPINE1; N6-methyladenosine (m^{6}A); demethylase

Submitted Dec 10, 2024. Accepted for publication Jan 16, 2025. Published online Jan 23, 2025.
doi: 10.21037/tcr-2024-2507
View this article at: https://dx.doi.org/10.21037/tcr-2024-2507

Introduction

In 2022, head and neck squamous cell carcinoma ranks eighth in global incidence of malignant tumors and tenth in mortality according to the most recent GLOBOCAN cancer statistics (1,2). Among patients with cancer of head and neck, the majority have head and neck squamous cell carcinoma (HNSCC) (3) and the worst prognosis belongs to those with hypopharyngeal squamous cell carcinoma (HSCC) (4), which represents approximately 3% of all cases (5) and shows a 5-year overall survival rate varying from 30% to 50% (6,7). Despite the recent progress in combination therapies, tumor recurrence and distant metastasis (e.g., to the lungs) remain areas of challenge in treating cancer of head and neck (3,8); hence, identification of novel therapeutic targets and prognostic indicators is highly desirable.

So far, more than 170 modifications of RNA have been identified (9). Among these, the most abundant modification in eukaryotic messenger RNA (mRNA) is the methylation of adenosine at position 6 (m^6A), which is recognized for its impact on precursor mRNA maturation, translation, and degradation process (10-12). The m^6A sites are mostly found in the 3'untranslated regions (UTR) close to stop codons and long internal exons (11,13). The m^6A methylation has dynamic and reversible characteristics realized by a series of methyltransferases ("writers"), demethylases ("eraser") and identifiers ("readers") (14). Previous studies in cancer showed that dysregulations in the expression of these m^6A regulatory proteins could act as promoters and suppressors of various biological processes in cancer (15), e.g., as promoters of tumorigenesis (16), tumor epithelial-mesenchymal transition (EMT) and metastasis (17), and suppressors of metastasis (18).

The fat mass and obesity-associated protein (FTO) gene is associated with obesity (19,20) and its protein is an RNA demethylase that catalyzes m^6A modification in nuclear mRNA (21). FTO plays an oncogenic role in acute myeloid leukemia (AML) (22,23), glioblastoma (24), melanoma (25), pancreas cancer (26,27), breast cancer (28,29), and cervical cancer (30), but a tumor-suppressor role in intrahepatic cholangiocarcinoma (31), lung cancer (32), bladder cancer (33,34), ovarian cancer (35), and colorectal cancer (36). This means that FTO has potentials as a therapeutic target for cancer therapy. Apart from results of a few studies that examined FTO in oral squamous cell carcinoma (OSCC) (37,38), little is known about the role played by FTO in HSCC. One study for OSCC found that FTO promoted progression of arecoline-induced OSCC by affecting proliferation, migration, and immune evasion mechanisms mediated by T-cells (38) and another one showed that FTO took part in the regulation of autophagy and tumorigenesis via targeting the gene encoding eukaryotic translation initiation factor gamma 1 (eIF4G1) (37). Thus, in the present study, our aim was to shed light on the functional roles of FTO in HSCC by focusing on its capacity as an RNA demethylase and how this affected tumor progression and metastasis.

At present, there are many studies on FTO in HNSCC, including nasopharyngeal cancer (39) and oropharyngeal (36,37) cancer. HSCC is a rare type of HNSCC with poor prognosis, and the mechanism of FTO in HSCC is rarely reported. In this study, we not only confirmed that FTO plays an important role in the proliferation and metastasis of hypopharyngeal cancer, but also found SERPINE1 as its downstream target gene for the first time. We present this article in accordance with the ARRIVE and MDAR reporting checklists (available at https://tcr.amegroups.com/article/view/10.21037/tcr-2024-2507/rc).

Highlight box

Key findings

- This study found that the fat mass and obesity-associated protein (FTO) played an oncogenic role in hypopharyngeal squamous cell carcinoma (HSCC) and was involved in epithelial-mesenchymal transformation.
- It was identified that SERPINE1 as a downstream target of FTO and demonstrated the direct influence of FTO on the m6A methylation process of SERPINE1 mRNA.

What is known and what is new?

- FTO promoted the proliferation, invasion and migration of hypopharyngeal cancer cells in vitro through demethylase action.
- SERPINE1 is identified as a downstream target of FTO-mediated m6A modification.
- FTO/SERPINE1 axis drives the tumorigenic properties of HSCC.

What is the implication, and what should change now?

- This study demonstrates that FTO-mediated RNA methylation plays a pivotal role in the progression of HSCC. Future research should focus on investigating the potential of FTO inhibitors as targeted therapeutic agents for HSCC.

Methods

Bioinformatics analysis

The UALCAN cancer database (http://ualcan.path.uab.edu/) was employed to examine the correlation between

FTO expression in normal tissues and tumors, utilizing clinical data from 44 non-cancerous tissues and 520 HNSCC tissues in January 2024. Gene Expression Profiling Interactive Analysis (GEPIA) website (http://gepia.cancer-pku.cn/) was employed to examine the protein expression of SERPINE1 in HNSCC and normal tissues, and to perform correlation analysis involving FTO and SERPINE1 in HNSCC. Additionally, the m^6A methylation site prediction was conducted using the Sequence-based RNA Adenosine Methylation Sites Predictor (SRAMP) website (http://www.cuilab.cn/sramp) (40).

Patients and samples

A sterile collection of tumor and non-cancerous tissues were collected from a cohort of 70 patients diagnosed with HSCC who underwent surgical resection at Shandong Provincial ENT Hospital between August 2013 and July 2015. Fresh specimens were promptly frozen in liquid nitrogen post-surgery and stored at –80 ℃. All the patients underwent surgery without receiving any preoperative radiotherapy or chemotherapy. The histopathological classification of each tumor specimen was confirmed by experienced pathologists. The study was conducted in accordance with the Declaration of Helsinki (as revised in 2013). The study was approved by Ethical Committee of Shandong Provincial ENT Hospital (No. 20210243) and informed consent was taken from all the patients.

Cell culture

The Human FaDu cell line was acquired from the American Type Culture Collection (ATCC, Manassas VA, USA HTB-43). Culturing of FaDu cells was carried out using Advanced Dulbecco's Modified Eagle's Medium/Nutrient Mixture F-12 Ham (DMEM/F12) (Gibco, Los Angeles, CA, USA), supplemented with 10% fetal bovine serum (FBS, BI, Israel). Cells were incubated in a controlled environment at 37 ℃ containing 5% CO_2.

Cell transfection and lentivirus infection

Small interfering RNAs (si-RNAs) targeting FTO and SERPINE1 were acquired from Gene Pharma (Suzhou, China). The specific sequences of the siRNAs used in this study were 5'-TCACCAAGGAGACTGCTATTT-3' (for si-FTO) and 5'-GCUCAGACCAACAAGUUCATT-3' (for si-SERPINE1). To achieve overexpression of FTO or SERPINE1, recombinant lentiviruses and plasmids containing the entire coding sequences of these genes were utilized. Furthermore, a mutant form of FTO lacking enzymatic activity due to two point-mutations (H231A and D233A) was inserted into the vector following the protocols described by Jia *et al.* (21) and Li *et al.* (22). Negative control was achieved by utilizing an empty lentivirus (Vector). Plasmids and siRNA were introduced into cells via Lipofectamine 3000 (Invitrogen, Waltham, MA, USA) following the guidelines provided by the manufacturer. Stable knockdown of FTO (shFTO) was achieved using lentiviruses purchased from Genechem (Shanghai, China) and non-targeting control shRNA (shNC) was used as a negative control.

RNA extraction and real-time PCR

Total RNA was extracted from the HSCC tissues or cell lines using TRIzol reagent (Invitrogen, CA, USA). The RevertAid First Strand cDNA Synthesis Kit (Thermo Fisher Scientific, MA, USA) was utilized for cDNA synthesis. PCR reactions were performed on Mastercycler® RealPlex 2 (Eppendorf, Hamburg, Germany) using TB Green® Premix Ex TaqTM (TaKaRa, Japan). The primer sequences can be found in *Table 1*. The relative expression of the target gene was determined using the comparative $2^{-\Delta\Delta Ct}$ method with Glyceraldehyde-3-phosphate dehydrogenase (GAPDH) as the internal control.

m^6A RNA methylation quantification

The relative m^6A level was assessed using the EpiQuik m^6A RNA Methylation Quantification kit (EpiGentek, Farmingdale, NY, USA). Briefly, after extracting total RNA from cells, 200 ng extracted total RNA was added to the wells. The capture antibody solution and the detection antibody solution were added respectively. Subsequently, the enhancer solution was added in accordance with the guidelines provided by the manufacturer. Finally, the OD value at 450 nm was assessed with a microplate reader (BioTek, VT, USA). The percentage of m^6A in the total RNA was calculated.

Western blotting analysis

Cells were lysed in RIPA buffer (Invitrogen, Carlsbad, CA, USA) and protein extraction was measured by the BCA assay (Beyotime, Shanghai, China). Equal amounts of protein were isolated using 10% SDS-PAGE, which

Table 1 Real-time PCR primer sequences

Genes	Forward primer	Reverse primer
FTL	TGGGCTTCTATTTCGACCGC	TTTCATGGCGTCTGGGGTTT
IFITM1	GCCAAGTGCCTGAACATCTG	TCACAGAGCCGAATACCAGT
DDIT4	AGACACGGCTTACCTGGATG	CGCAGTAGTTCTTTGCCCAC
JAK3	CTCTATGCCTGCCAAGACCC	GGCACCTGTATTGTCGCCTA
SERPINE1	TTGGTGAAGGGTCTGCTGTG	GGGTGAGAAAACCACGTTGC
DKK3	TCGATGATGCACTCGTGGCT	TCGATGATGCACTCGTGGCT
CPT1C	AAGAGTTGCTGCCTGACTGG	CCCACAAACACGAGGCAAAC
IFI27	TGGCCAGGATTGCTACAGTTG	TATGGAGGACGAGGCGATTC
IFI6	CTGATGAGCTGGTCTGCGAT	ATACTTGTGGGTGGCGTAGC
COL7A1	ACCTGCACGCGCCTTTA	CGAACTCTGTCCGTGGGTCA
FTO	CGAGAGCGCGAAGCTAAGA	GCTGCCACTGCTGATAGAAT
GAPDH	ACCCAGAAGACTGTGGATGG	TCTAGACGGCAGGTCAGGTC

PCR, polymerase chain reaction.

were then transferred on polyvinylidene fluoride (PVDF) membranes (Thermo Fisher Scientific, MA, USA). The membranes were subjected to overnight incubation at 4 ℃ with primary antibodies, followed by a subsequent incubation with secondary antibody (1:10,000, ZhongShan-Golden Bridge, Beijing, China) for 2 hours at room temperature. Bands were visualized using a ChemiDoc™ imaging system (Bio-Rad, Hercules, CA, USA). Primary antibodies included anti-FTO (1:1,000, Cell Signaling Technology, USA #4393), anti-SERPINE1 (1:500 Abcam, UK ab317604), anti-GAPDH (1:10,000, ZhongShan-Golden Bridge, Beijing, China TA309157), anti-E-cadherin (1:1,000, Cell Signaling Technology, USA #3195), anti-N-Cadherin (1:1,000, Cell Signaling Technology, USA #13116), anti-Snail (1:1,000, Cell Signaling Technology, USA #9585). The protein bands were scanned utilizing a Clinx Science Instrument and were analyzed using the Image J software.

Wound healing assay

A 6-well plate was populated with cultured cells until they reached a confluence of over 90%. A sterile pipette tip measuring 200 µL was employed to create an incision on the cell layer, resulting in the formation of a wound. The process of wound healing was observed by utilizing a light microscope in an inverted position, and the closure of the gap was documented at both 0 and 48 hours. The assessment of wound closure speed was conducted through the utilization of Image J software.

Migration and invasion assays

The upper chamber was initially populated with 2×10^4 cells, which were cultured in 200 µL of serum-free Dulbecco's modification of Eagle's medium Dulbecco (DMEM). In contrast, the lower chamber contained 600 µL of DMEM supplemented with 20% Foetal Bovine Serum (FBS). Cell invasion assays were performed utilizing an 8 mm Matrigel invasion chamber (BD Bioscience, Franklin Lakes, New Jersey, USA) and the migration assays did not utilize any adhesive matrix. After 36 or 48 h incubation, the cells that passed through the filter were immobilized on the underside using a 4% paraformaldehyde solution, were subjected to staining with a 0.1% crystal violet solution, and subsequently were enumerated and captured in photographs.

Cell viability assay

A 96-well plate was used to seed a population of control and transfected cells, with a density ranging from 4,000 to 5,000 cells. Subsequently, 10 µL of reagent from the Cell Counting Kit-8 (CCK-8, Dojindo, Kumamoto, Japan) was added for cell proliferation assays at 24, 48, 72 or 96 h following the manufacturer's protocol. The

absorbances were detected at 450 nm by using a microplate reader (BioTek, VT, USA). The ethynyl deoxyuridine (EdU) assay (EdU kit, RiboBio, Guangzhou, China) was also used to assess the cell viability according to the manufacturer's instructions.

Tumor xenografts in nude mice

Male BALB/c nude mice (4–5 weeks) were purchased from Vital River Laboratory Animal Technology (Beijing, China). The experimental mice were acclimated for one week under standard controlled conditions (22±2 ℃, 45–55% humidity). The mice were divided into four groups in a random manner (n=7 per group) use the random number table method. In two groups, shFTO or shNC FaDu cells (1×10^6 cells/mouse) were inoculated subcutaneously into nude mice. Tumorigenesis was observed every other day and calculated according to the following formula: Volume (mm^3) = (length × $width^2$)/2. After 5 weeks of incubation, the mice were euthanized using carbon dioxide exposure, and the tumors were removed, preserved in 4% paraformaldehyde for 24 hours at ambient temperature, and subsequently embedded in paraffin for immunohistochemical (IHC) staining. In other two intravenous mice model groups, cells were respectively injected into the lateral tail vein (n=7 per group). All mice were euthanized eight weeks after injection, and their lungs were collected and preserved in 4% paraformaldehyde. The lung tissues were then embedded in paraffin for subsequent IHC staining. Animal experiments were performed according to the Guide for the Care and Use of Laboratory Animals of the National Research Council (8^{th} edition), and were approved by the Ethics Committee of Shandong Provincial ENT Hospital (No. 20210213). A protocol was prepared before the study without registration.

Hematoxylin and eosin (H&E) and IHC staining

IHC staining was conducted following the previously established protocol (41). The tissues were sliced into slides with a thickness of 2 μm. The slides underwent dewaxing and were subsequently stained using standard procedures for H&E staining. In order to perform IHC staining, the tissue slides were deparaffinized and subjected to antigen retrieval. Then, the slides were blocked and processed. The primary antibody was applied onto the slides, followed by the secondary antibody incubation. Two experienced pathologists independently evaluated the specimens in a blinded manner. The evaluation was based on the staining intensity (0 for no staining, 1 for 1–25% stained, 2 for 26–50% stained, and 3 for 51–100% stained) and the percentage of positive cells (0 for 0–5%, 1 for 6–25%, 2 for 26–50%, 3 for 51–75%, and 4 for >75%).

Me-RIP assay

The MeRIP m^6A Transcriptome Profiling Kit (Ribo, Guangzhou, China) was utilized for the implementation of Me-RIP. In brief, the RNA fragmentation buffer was employed to fragment a total of 100 μg RNA from shNC and shFTO samples. Then, a portion of the fragmented RNA (approximately 10%) was excluded as input. The Me-RIP reaction solution was prepared according to the manufacturers protocol. The anti-m^6A antibody (5 μg) was applied to coat magnetic beads A/G. The Me-RIP reaction solution was then subjected to incubation with the anti-m^6A magnetic beads for a duration of 2 hours at a temperature of 4 ℃. After undergoing multiple rounds of cleansing and various protocols, the methylated RNA was isolated utilizing the Magen Hipure Serum/plasma miRNA Kit (Magen, Guangzhou, China). For MeRIP-qPCR, the methylated RNA purified by the above steps was reverse-transcribed and qPCR was performed. The primer sequences utilized in this experiment are provided in *Table 2*.

Transcriptome-sequencing (RNA-seq)

RNA-seq was conducted by RuizhiBio Co., Ltd. (Jinan, China). Total RNA from shFTO and shNC FaDu cells were extracted with TRIzol. rRNA was removed from the total RNA and libraries were prepared for RNA sequencing. The Illumina HiSeq platform with 150 bp paired-end mode was utilized to conduct the RNA-seq analysis.

Statistical analysis

All data analysis was performed by SPSS version 22.0 (SPSS, Chicago, IL, USA). Data were presented as mean ± standard deviation (SD) or median with 95% confidence interval (CI). According to the characteristics of the data, unpaired *t*-test, one-way analysis of variance (one-way ANOVA), Chi-square test or rank sum test was conducted to compare data between groups. Log-rank (Mantel-Cox) test was used to analyze the survival of HSCC patients. The Pearson correlation test was employed to conduct the analysis of correlations. The statistical significance was set as P values <0.05.

Table 2 MeRIP-qPCR primer sequences

Genes	Forward primer	Reverse primer
SERPINE1-M^{6}A-1	TTCATGCCCCACTTCTTCAGG	GGCTCCTTTCCCAAGCAAGTT
SERPINE1-M^{6}A-2	CCGATGGCCATTACTACGACA	GAATGTTGGTGAGGGCAGAGA
SERPINE1-M^{6}A-3	ACTGGAAAGGCAACATGACCA	ATGTCGGTCATTCCCAGGTTC
SERPINE1-M^{6}A-4	CAGCTGTCATAGTCTCAGCCC	TCCATCACTTGGCCCATGAAA
SERPINE1-M^{6}A-5	TTCATGGGCCAAGTGATGGAA	CTTTCCCGATGCATCTCCAGT
SERPINE1-M^{6}A-6	ACTGGAGATGCATCGGGAAAG	GCCAAGGTCTTGGAGACAGAT
SERPINE1-M^{6}A-7	TTCAGGGGATCAAAAGGACGG	CCCCTTGCATTTCTGCTCCTA
SERPINE1-M^{6}A-8	TAGGAGCAGAAATGCAAGGGG	GGCTGTGAGTCACCCTGTAAT

MeRIP-qPCR, methylated RNA immunoprecipitation quantitative polymerase chain reaction.

Results

FTO expression is elevated in HSCC tissues and is associated with HSCC prognosis

As the first step in our exploration of the role played by FTO in HNSCC/HSCC, we analyzed data from the UALCAN database. Analysis showed that, first, FTO expression was aberrantly upregulated in HNSCC tissues compared to normal tissues (*Figure 1A*). Second, for HNSCC, positive associations were found between elevated FTO expression and tumor grade, individual cancer stages, and lymph node metastasis (*Figure 1B-1D*). Third, comparing HSCC tumor tissues and their adjacent non-cancerous tissues, it was found that in tumor tissues FTO was significantly upregulated (RT-qPCR analysis of FTO mRNA; *Figure 1E*), and the expression of FTO protein was higher in both Western blot analysis (*Figure 1F*, Figure S1) and in IHC staining analysis (in *Figure 1G*, FTO protein was primarily localized within nuclei of cancer cells; also see *Figure 1H*). Fourth, Kaplan-Meier analysis showed that patients with HSCC with elevated FTO protein expression had significantly lower overall survival compared to those with lower FTO protein expression levels (*Figure 1I*). All in all, these findings strongly suggested that FTO was upregulated in patients with HSCC, where it potentially contributed to the initiation and progression of HSCC.

Knockdown of FTO inhibits the proliferation, migration, and invasion of HSCC cells in vitro

To explore the functional significance of FTO in HSCC, FaDu cells were subjected to a loss-of-function study for the progression of HSCC by transfecting them with si-RNA specifically designed to target FTO. The efficiency of FTO knockdown was assessed using RT-qPCR and Western blot analysis. Our findings revealed a substantial reduction in both mRNA and protein expression levels within FaDu cells (*Figure 2A,2B*). We examined the level of relative m^{6}A content to total RNAs in FaDu cells and found that the reduction of FTO led to an increase in global m^{6}A modification levels within FaDu cells (*Figure 2C*). Furthermore, knockdown of FTO resulted in significant reductions in (I) the proliferative capacity (*Figure 2D*), (II) the cell viability (EdU labeling assay; *Figure 2E*), and (III) the migration and invasiveness capabilities (*Figure 2F*) of HSCC cells. In the next step, we investigated how FTO knockdown affected EMT in HSCC by examining the protein expression of E-cadherin, N-cadherin and Snail, which are the key markers associated with EMT. Thus, Western blot analysis showed that in FTO-silenced FaDu cells, the expression of E-cadherin was increased, but that of N-cadherin and Snail expression was decreased (*Figure 2G*). Taken together, these results suggested that FTO took part in the proliferation, migration, invasion, and EMT of HSCC cells, which might be through its function as an m^{6}A demethylase.

The oncogenic function of FTO is dependent on m^{6}A RNA demethylase activity

In order to investigate whether the effects observed for FTO knockdown were attributed to FTO demethylase function, FaDu cells were transfected with lentivirus carrying wild-type FTO (FTO-WT) and mutant FTO (FTO-mut), which contained two point-mutations (H231A

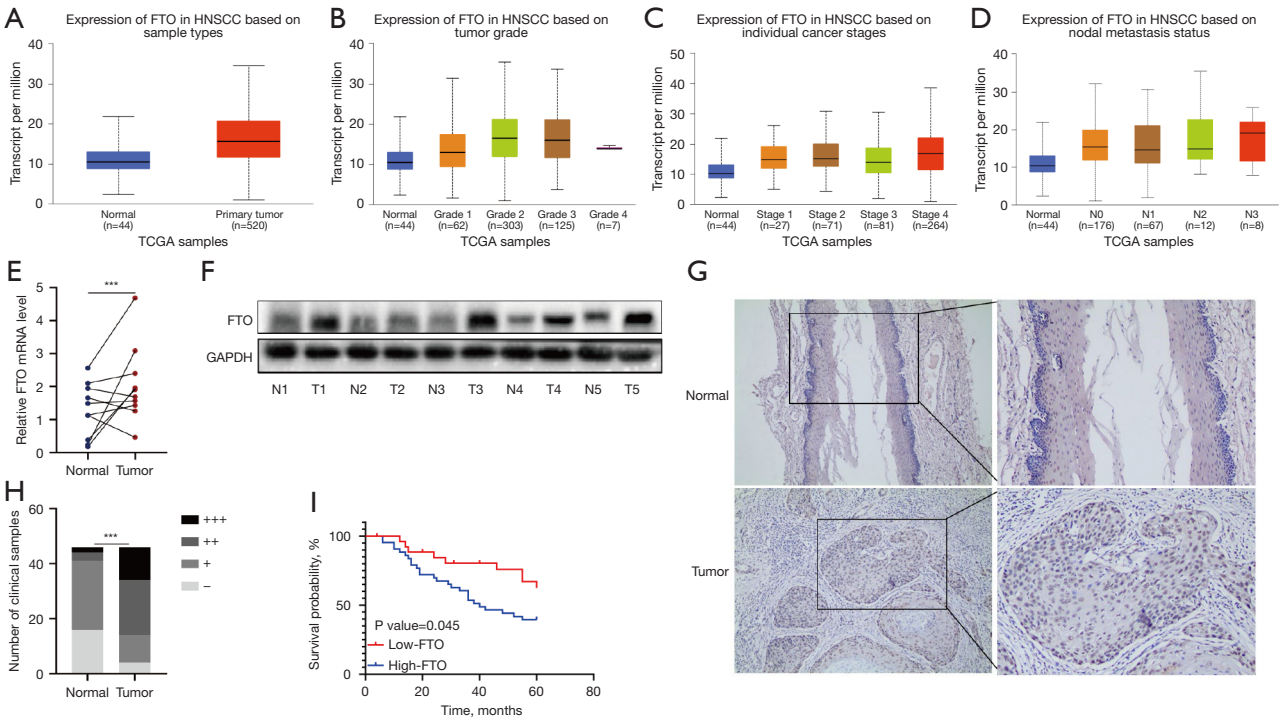

Figure 1 FTO expression is elevated in HNSCC/HSCC tissues and predicts poor prognosis for patients with HSCC. (A) Boxplot showing relative expression of FTO in normal (n=44) and HNSCC tissues (n=520) extracted from the UALCAN database. (B-D) In HNSCC, elevated FTO expression was correlated with tumor grade, individual cancer stages and lymph node metastasis. (E) The mRNA expression levels of FTO in the HSCC tissues were compared to those in corresponding non-cancerous tissues (n=10). (F) Western blot assay of FTO expression in five paired of HSCC tissues. (G) Representative IHC images of FTO expression in HSCC tumor and non-tumor tissues. Left: magnification, 10×; right: magnification, 20×. (H) Expression of FTO was quantitatively analyzed according to the staining score. –, negative; +, weakly positive; ++, positive; +++, strongly positive. (I) Kaplan-Meier survival curve for the overall survival of the patients with HSCC based on their FTO protein levels as determined by IHC score. ***, P<0.001. FTO, fat mass and obesity-associated protein; HNSCC, head and neck squamous cell carcinoma; TCGA, The Cancer Genome Atlas; GAPDH, glyceraldehyde-3-phosphate dehydrogenase; HSCC, hypopharyngeal squamous cell carcinoma; UALCAN, The University of ALabama at Birmingham CANcer data analysis Portal; IHC, immunohistochemical.

and D233A) that eliminated the enzymatic activity of FTO (19,20). The Western blot analysis showed that the expression of FTO was significantly higher in FTO-WT and FTO-mut FaDu cells compared to the control (i.e., FaDu cells with empty lentivirus), thus confirming the transfection efficiency of FTO (*Figure 3A*). CCK8 assays revealed that the proliferation of FaDu cells was significantly enhanced upon overexpression of FTO, while no impact on proliferation was observed in FTO-mut FaDu cells lacking the demethylation domain (*Figure 3B*). While FTO-WT overexpression increased cell migration and invasion capabilities compared to control, there was no significant alteration in the phenotype upon forced expression of the mutant variant using FTO-mut (*Figure 3C,3D*). Taken together, these findings strongly suggested that the oncogenic role played by FTO was dependent on its m^{6}A demethylase activity.

SERPINE1 is identified as a downstream target of FTO-mediated m^{6}A modification

To investigate the potential downstream targets of FTO in HSCC, we conducted RNA-seq analysis on our stable FaDu cells with FTO knockdown (shFTO). We identified highly influential genes based on a fold-change >2 and an adjusted P value <0.05. We also observed significant downregulation of 680 genes and upregulation of 751 genes in FTO-knockdown cells compared to control (*Figure 4A*).

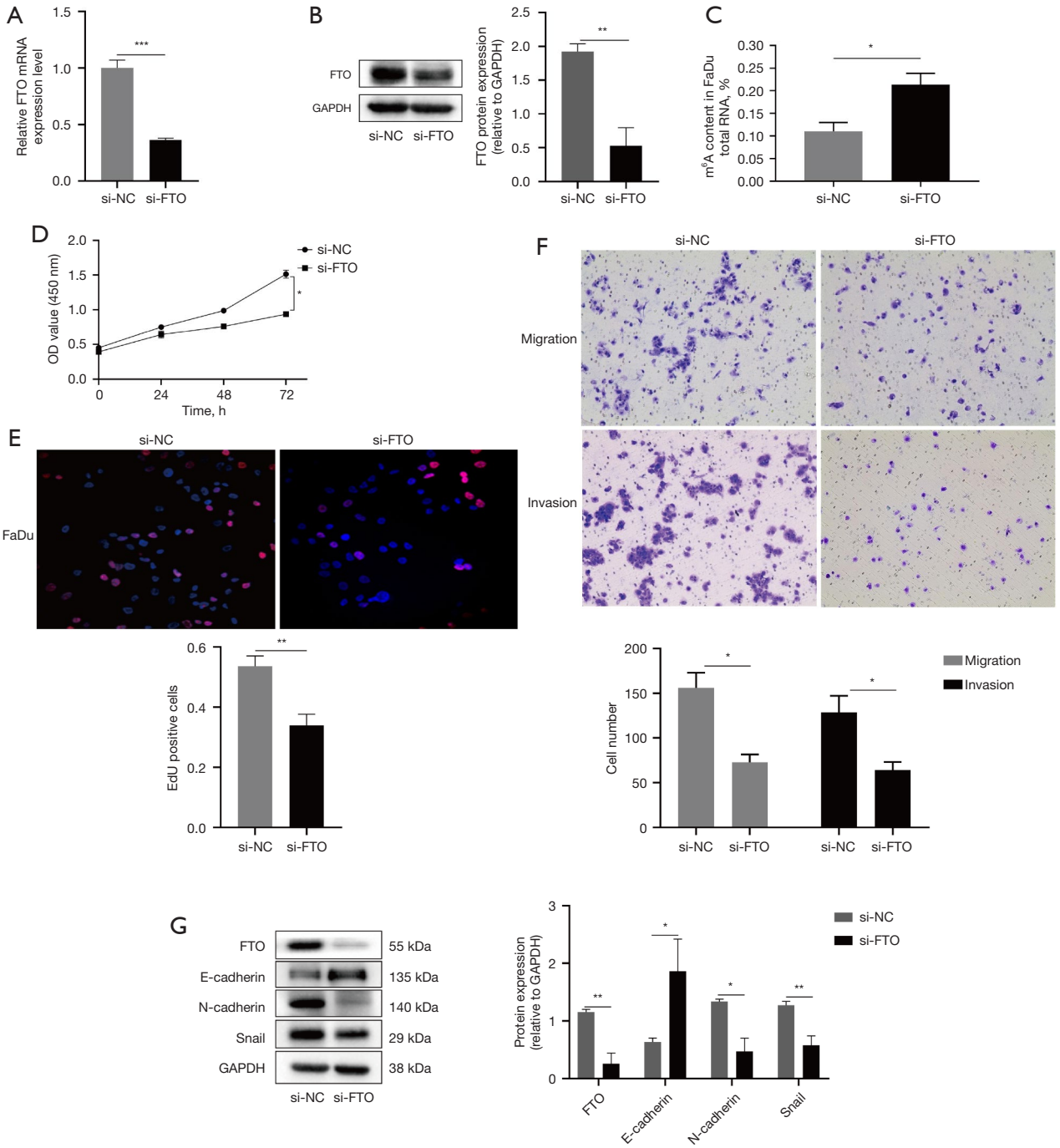

Figure 2 Knockdown of FTO inhibited the proliferation, migration and invasion of HSCC cells *in vitro*. (A,B) The levels of FTO mRNA and protein were assessed in FaDu cells following transfection with FTO-siRNA. (C) The relative m^{6}A content to total RNA measured in FTO-knockdown FaDu cells. (D) The effect of FTO down-regulation on cell growth was detected by CCK8 assay in FTO-knockdown FaDu cells. (E) EdU analysis of cell proliferation in FTO-knockdown FaDu cells (magnification, 10×). (F) Cell migration and invasion assays were performed in FTO-silenced FaDu cells by crystal violet staining (magnification, 10×). (G) Western blot analysis was performed to examine the protein expression of EMT-related markers in FTO-silenced FaDu cells. *, P<0.05; **, P<0.01; ***, P<0.001. FTO, fat mass and obesity-associated protein; NC, negative control; GAPDH, glyceraldehyde-3-phosphate dehydrogenase; OD, optical density; CCK8, Cell Counting Kit-8; EMT, epithelial-mesenchymal transformation.

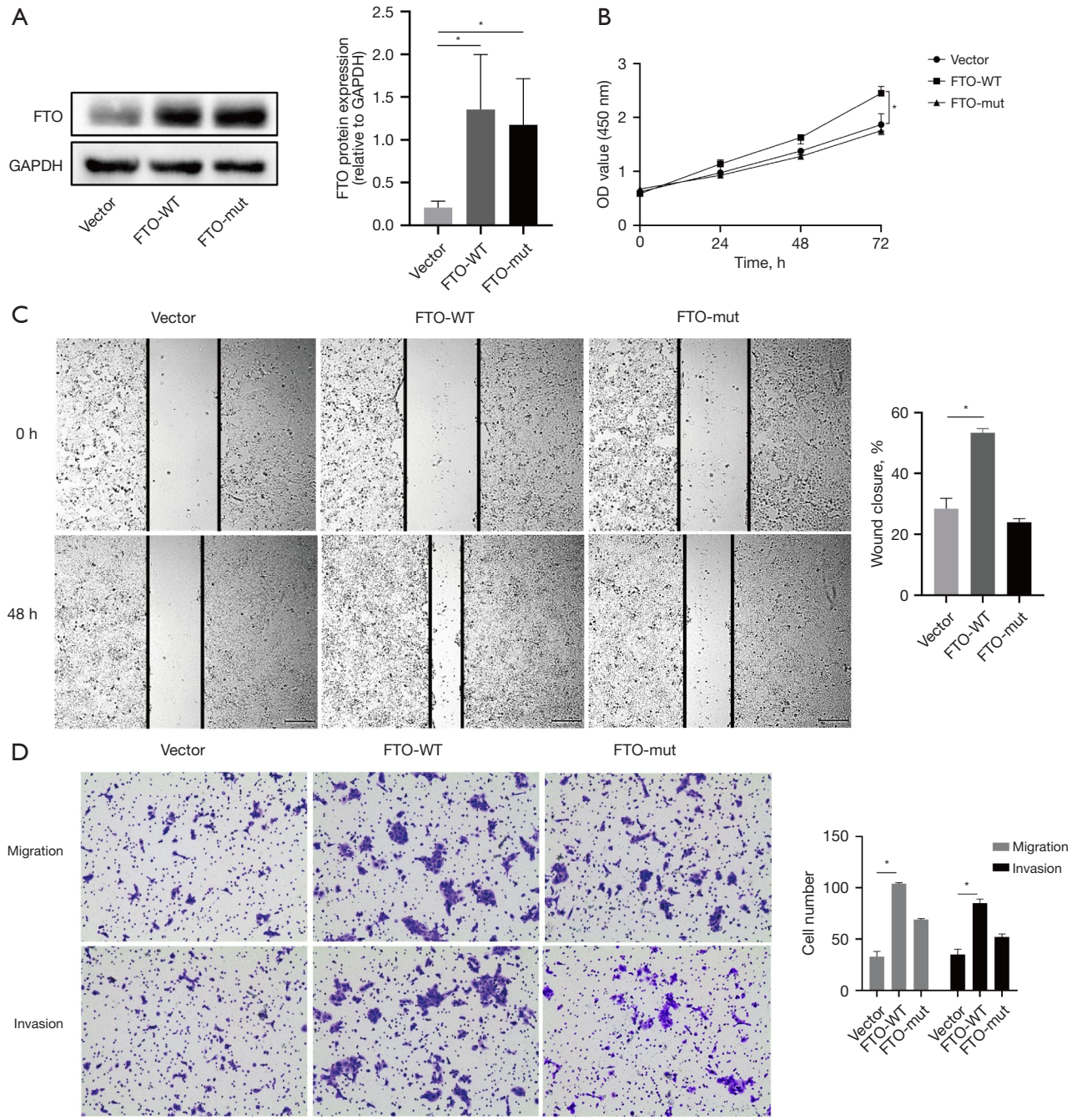

Figure 3 The oncogenic function of FTO is dependent on m^{6}A RNA demethylase activity. (A) Enforced FTO-WT and FTO-mut expression in FaDu cells. (B) CCK8 analysis of cell proliferation in FaDu cells transfected with FTO-WT and FTO-mut plasmids. (C) Wound healing assay: the healing percent and migration of cells were measured at 48 h after transfection with FTO-WT and FTO-mut overexpression plasmids (magnification, 4×). (D) Analysis of cell migration and invasion capacity in FTO-WT and FTO-mut FaDu cells by crystal violet staining (magnification, 10×). *, P<0.05. FTO, fat mass and obesity-associated protein; GAPDH, glyceraldehyde-3-phosphate dehydrogenase; WT, wild-type; mut, mutant; OD, optical density; CCK8, Cell Counting Kit-8.

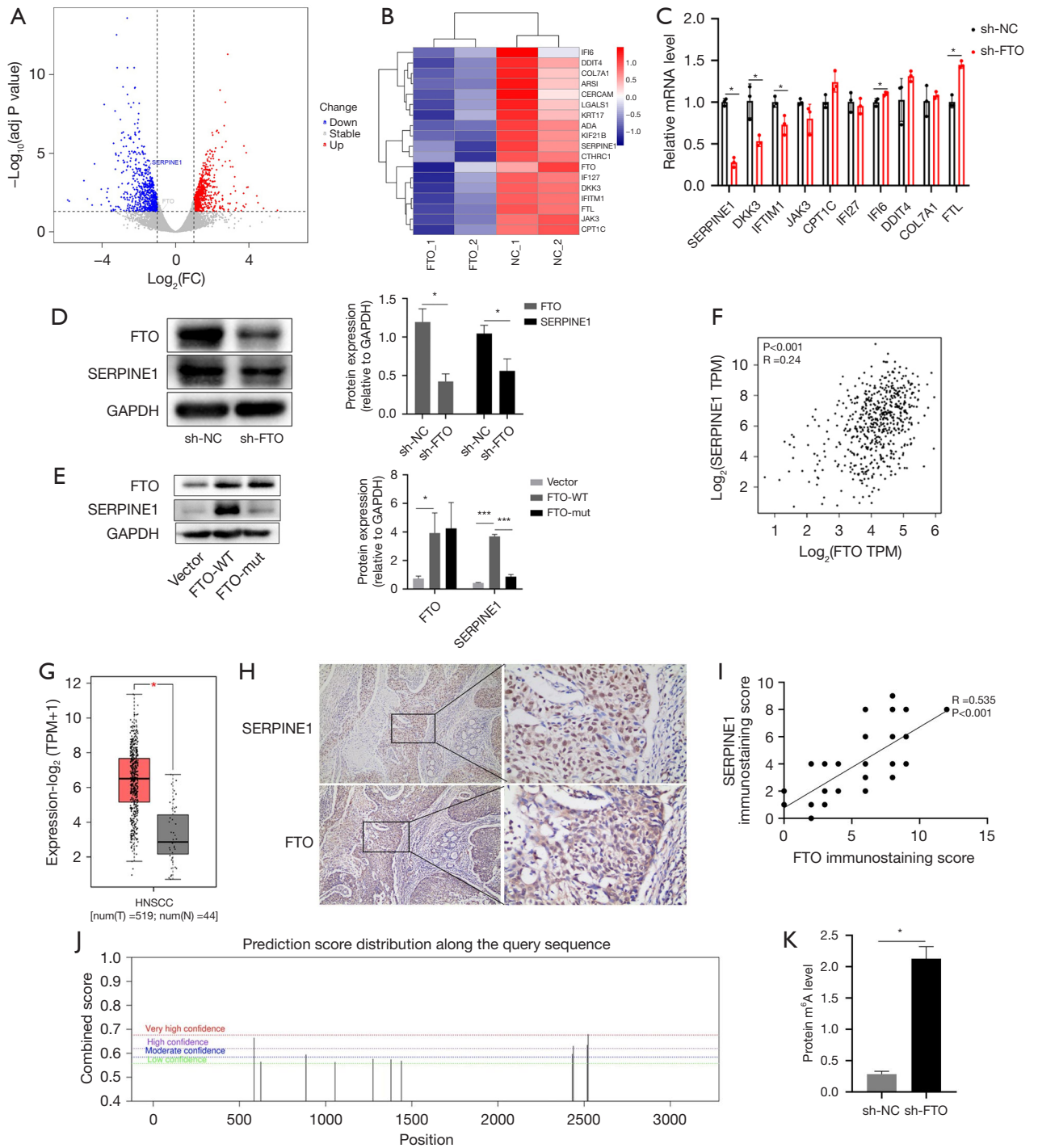

Figure 4 SERPINE1 is identified as a downstream target of FTO-mediated m^{6}A modification. (A) Volcano diagram of DEGs with P<0.05. (B) Heatmap of the expression of the significantly downregulated genes, which were closely related to HNSCC. (C) RT-qPCR assays were used to detect the RNA expression levels of 10 DEGs in stable FTO-knockdown FaDu cells. (D) SERPINE1 protein expression was significantly down-regulated in stable FTO-knockdown FaDu cells. (E) SERPINE1 expression was significantly up-regulated in FaDu cells transfected with FTO-WT plasmids, but not in those transfected with FTO-mut plasmids. (F) The scatter plot showing the expression of FTO and SERPINE1 in HNSCC patients (data from GEPIA, R=0.24, P<0.001). (G) Using data of GEPIA database, the expression of SERPINE1 was found to be significantly increased in HNSCC when compared to normal epithelial tissues (P<0.05). (H) The colocalization

of FTO and SERPINE1 expression in consecutive sections of HSCC tissues by IHC. Left: magnification, 10×; right: magnification, 40×. (I) The expression correlation analysis of SERPINE1 and FTO in hypopharyngeal cancer tissues based on immunohistochemistry analysis. (J) Potential sites for m^6A modification in the sequence of SERPINE1 gene using SRAMP database. (K) MeRIP-qPCR showed knockdown of FTO increased m^6A modification in SERPINE1. *, P<0.05; ***, P<0.001. FC, fold change; NC, negative control; FTO, fat mass and obesity-associated protein; GAPDH, glyceraldehyde-3-phosphate dehydrogenase; WT, wild-type; mut, mutant; TPM, transcripts per million; HNSCC, head and neck squamous cell carcinoma; DEGs, differentially expressed genes; RT-qPCR, real-time quantitative polymerase chain reaction; IHC, immunohistochemical; GEPIA, Gene Expression Profiling Interactive Analysis; SRAMP, Sequence-based RNA Adenosine Methylation Sites Predictor; MeRIP-qPCR, methylated RNA immunoprecipitation quantitative polymerase chain reaction.

We identified and visualized a panel of ten differentially expressed genes (DEGs) implicated in the pathogenesis of HNSCC using a heat map representation (*Figure 4B*). Subsequently, RT-qPCR was utilized to assess the levels of expression for ten DEGs in cells with FTO knockdown. The results revealed that the most marked decrease in DEGs in our stable FTO-knockdown FaDu cells belonged to SERPINE1 (*Figure 4C*). Western blot assay showed that knockdown of FTO in FaDu cells significantly suppressed SERPINE1 expression (*Figure 4D*) and overexpression of FTO enhanced SERPINE1 expression, but forced expression of the mutant had no effect (*Figure 4E*). Analysis of data from GEPIA database also demonstrated a positive correlation between the expression levels of FTO and SERPINE1 (R=0.24, P<0.001) (*Figure 4F*), where it was found that HNSCC tissues showed significant upregulation of SERPINE1 compared to normal tissues (T=519, N=44, P<0.05) (*Figure 4G*). Additionally, to elucidate the association between SERPINE1 and FTO in HSCC tissues, IHC staining was performed. Consistent with the database analysis, co-localization of SERPINE1 expression with FTO expression was observed in consecutive sections of HSCC tissues (R=0.535, P<0.001) (*Figure 4H,4I*). Thus, these results indicated that, first, FTO regulated the expression of SERPINE1 *in vitro*, and second, a positive association existed between the levels of SERPINE1 and FTO in clinical samples.

To verify SERPINE1 as a potential target of FTO for m^6A modification, we employed the SRAMP database (http://www.cuilab.cn/sramp) to forecast multiple methylation binding sites of SERPINE1 modified by FTO (*Figure 4J*). Then, we conducted an m^6A-RNA immunoprecipitation experiment and utilized RT-qPCR to analyze the results. As expected, the enrichment of SERPINE1 was significantly increased in the third site of FTO-knockdown FaDu cells (*Figure 4K*). In summary, our results confirmed that SERPINE1 was a downstream target of FTO-mediated m^6A modification.

Silencing SERPINE1 inhibits the cell proliferation, migration and invasion of FaDu cells

To evaluate the biological function of SERPINE1 knockdown in FaDu cells, siRNAs against SERPINE1 were synthesized, and the silencing efficiency of SERPINE1 by siRNA was verified by PCR and Western blot assays in FaDu cells (*Figure 5A,5B*). As expected, SERPINE1 knockdown significantly reduced cell viability, migration, and invasion in FaDu cells (*Figure 5C-5E*). To further analyze the effects of SERPINE1 on EMT in HSCC, the expression of EMT markers including E-cadherin, N-cadherin and Snail were determined by Western blot analysis. The results showed that the expression of E-cadherin was increased, whereas that of N-cadherin and Snail was decreased in SERPINE1-silenced FaDu cells (*Figure 5F*). Altogether, these data suggested that the silencing of SERPINE1 expression attenuated proliferation, migration, and invasion via EMT pathway in HSCC cells.

Overexpression of SERPINE1 partially rescues the inhibitory effect of FTO knockdown on the malignancy of FaDu cells

To determine the effects of the coordination between FTO and SERPINE1 on the biological function of HSCC cells, we overexpressed SERPINE1 (OE-SERPINE1) in stable FTO knockdown (shFTO) cells and performed a series of restoration assays. Western blot analysis confirmed that SERPINE1 protein expression was significantly elevated in FaDu cells using the lentiviral approach (*Figure 6A*). Moreover, it was found that overexpression of SERPINE1 reversed effects of stable FTO silencing on cell proliferation (CCK-8 assay; *Figure 6B*), migratory and invasive capabilities (wound healing assay in *Figure 6C* and transwell assay in *Figure 6D*, respectively), and EMT process (*Figure 6E*) in HSCC cells. Thus, these results indicated that SERPINE1 overexpression could significantly alleviate the inhibitory effects of FTO knockdown on HSCC cell

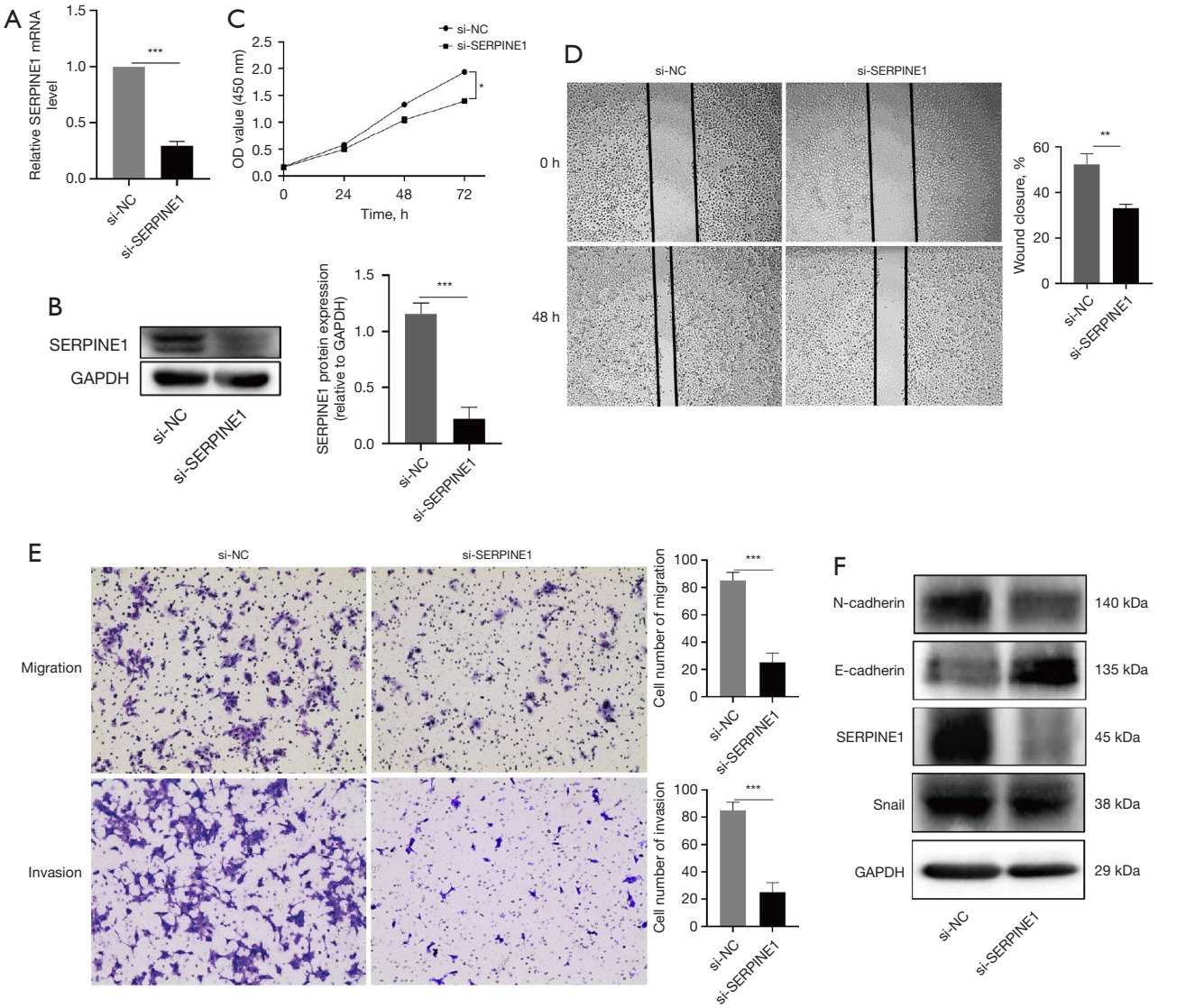

Figure 5 Silencing SERPINE1 inhibits the cell proliferation, migration, and invasion of FaDu cells. (A,B) The transfection efficiency of SERPINE1 in FaDu cells was validated through RT-qPCR and Western blot analysis. Effects of silencing SERPINE1 on proliferation, migration, and metastasis in FaDu cells were examined by (C) CCK8 cell viability, (D) wound-healing assay (magnification, 4×), and (E) transwell migration and invasion stained by crystal violet (magnification, 10×). (F) The expression of EMT-related proteins in SERPINE1-silenced FaDu cells were examined by Western blot. *, P<0.05; **, P<0.01; ***, P<0.001. RT-qPCR, real-time quantitative polymerase chain reaction; NC, negative control; OD, optical density; GAPDH, glyceraldehyde-3-phosphate dehydrogenase; CCK8, Cell Counting Kit-8.

proliferation, migration, and invasion, and mediated the reversal of EMT.

Silencing FTO inhibits HSCC tumor growth and metastasis in vivo

To further validate the oncogenic role of FTO in HSCC, we conducted an *in vivo* subcutaneous implantation experiment to investigate the impact of FTO knockdown on HSCC tumorigenicity. We observed that shFTO effectively suppressed HSCC tumor growth in nude mice, as evidenced by the significant reduction in both tumor size and weight compared to the negative control (shNC) group (*Figure 7A-7C*). Moreover, when stable FTO-knockdown

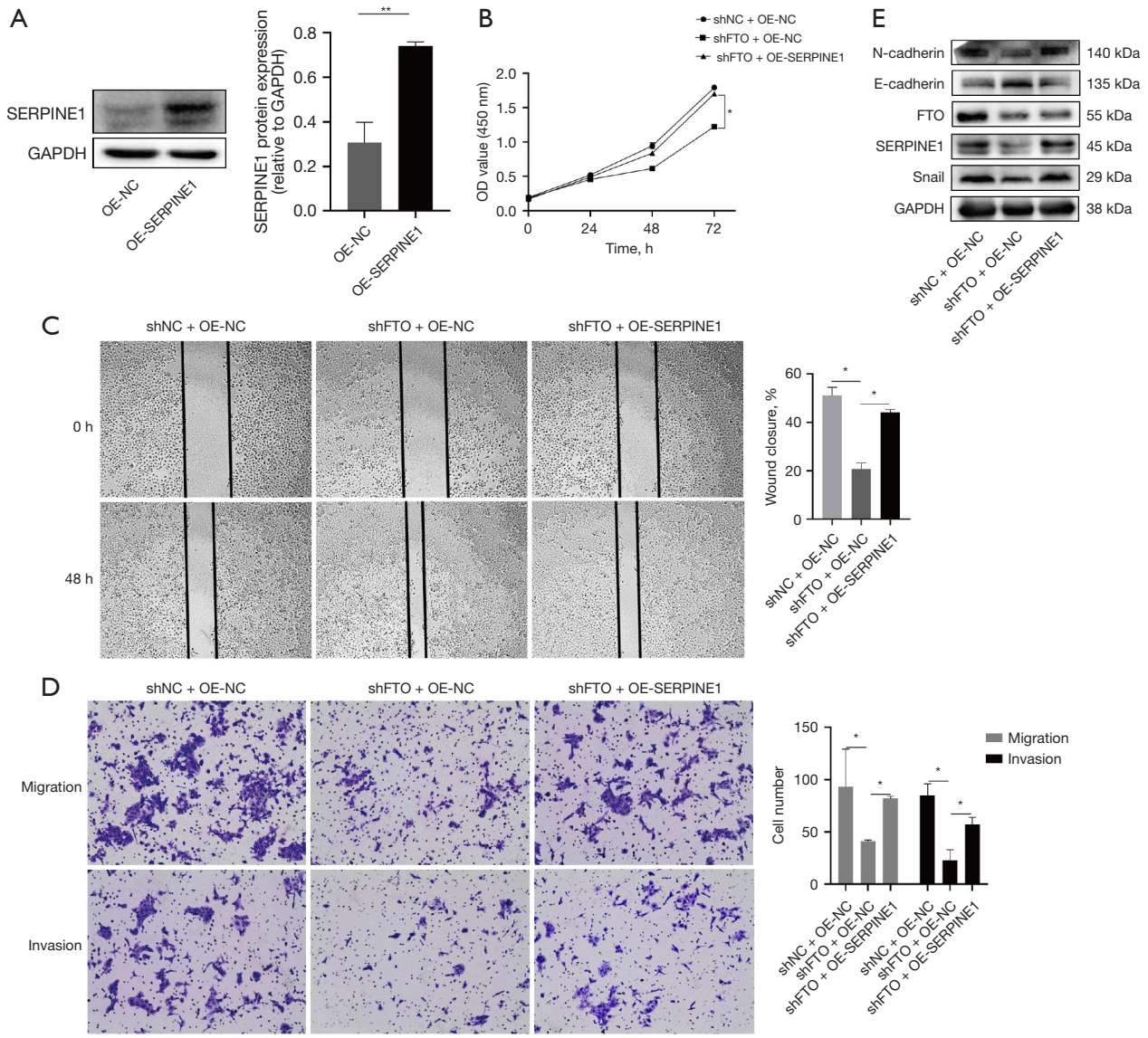

Figure 6 Overexpression of SERPINE1 partially rescues knockdown of FTO-inhibited malignancy of FaDu cells. (A) The efficiency of the up-regulated SERPINE1 expression was verified by Western blot. (B) CCK8 assay confirmed that upregulation of SERPINE1 could restore the inhibitory effect of FTO knockdown on FaDu cells. (C,D) The migration and invasion abilities of FaDu cells were restored by SERPINE1 up-regulation by crystal violet staining. Wound-healing (magnification, 4×). Transwell (magnification, 10×). (E) SERPINE1 reversed the stable knockdown of FTO-attenuated EMT of HSCC cells. *, P<0.05; **, P<0.01. GAPDH, glyceraldehyde-3-phosphate dehydrogenase; OE, over expression; NC, negative control; OD, optical density; FTO, fat mass and obesity-associated protein; CCK8, Cell Counting Kit-8.

FaDu cells were injected into nude mice via tail vein injection, we observed a remarkable inhibition of lung metastasis along with fewer lung metastatic tumors (*Figure 7D-7F*). IHC assays also revealed that FTO knockdown upregulated E-cadherin expression and downregulated N-cadherin expression, which were indicative of its inhibitory effect on tumor EMT process (*Figure 7G*). Collectively, these results suggested that FTO played a critical role in promoting both HSCC tumor growth and metastasis *in vivo*.

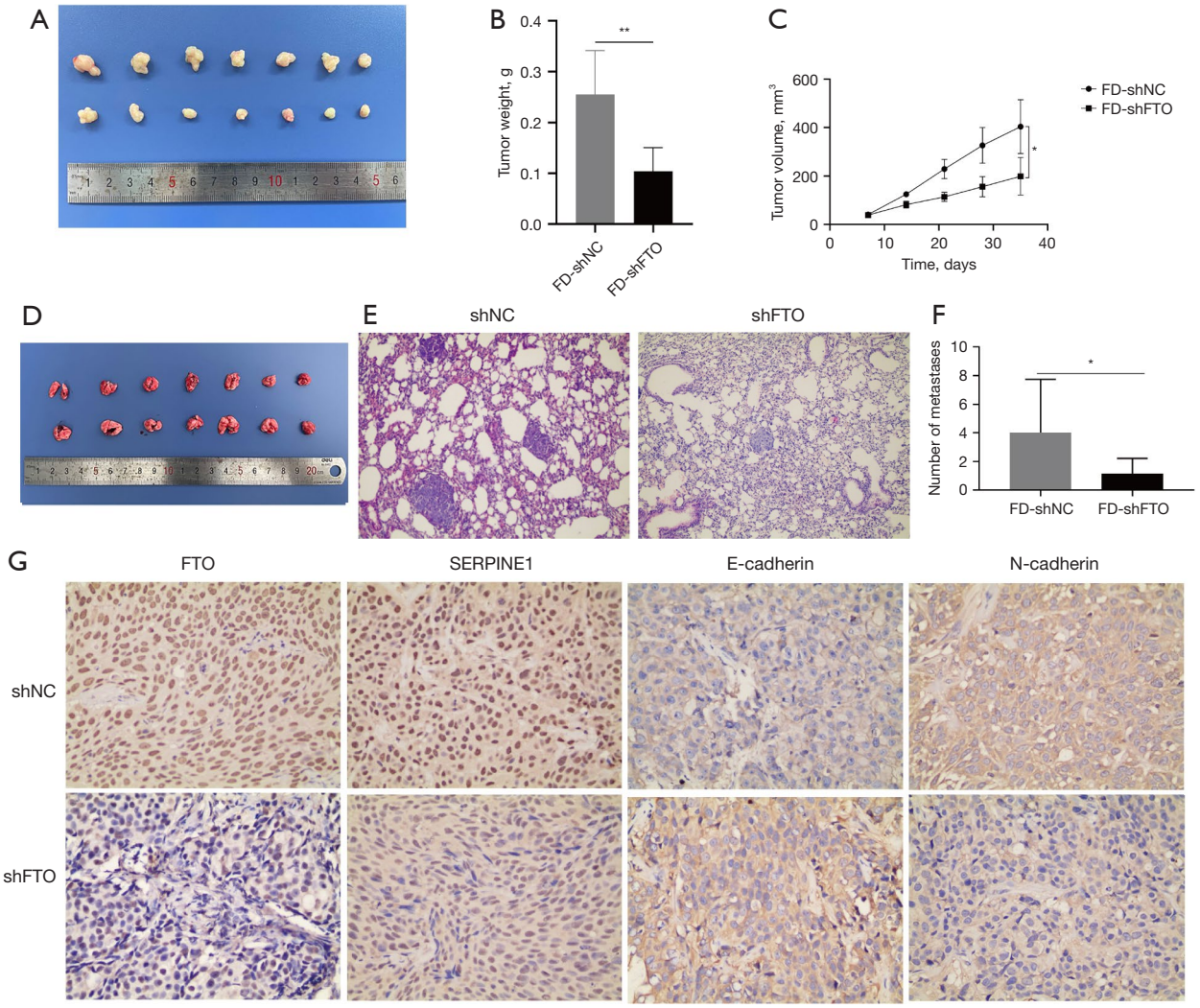

Figure 7 Silencing of FTO inhibits HSCC tumor growth and metastasis *in vivo*. (A) Representative illustration of subcutaneous tumors extracted from a mouse model with FaDu cells transfected with shNC and shFTO (n=7). (B) Tumor weights and (C) volumes were assessed post-excision from nude mice in the experimental groups. (D) Representative image of metastatic lung tumors is shown (n=7). (E) The metastases were confirmed by H&E staining (magnification, 10×). (F) The number of lung tumors was quantitatively analyzed. (G) The expression of FTO, SERPINE1, N-cadherin and E-cadherin was analyzed by IHC for shNC and shFTO FaDu-derived xenografts (magnification, 40×). *, P<0.05; **, P<0.01. FD, FaDu; NC, negative control; FTO, fat mass and obesity-associated protein; HSCC, hypopharyngeal squamous cell carcinoma; H&E, hematoxylin and eosin; IHC, immunohistochemical.

Discussion

Previous studies in cancer showed that FTO may play an oncogenic role (24-30) or a tumor-suppressor role (31-36) depending on the type of malignancy. For example, in AML, FTO promoted leukemogenesis by reducing m^6A levels in mRNA transcripts ASB2 and RARA (22), and in breast cancer, the FTO-mediated progression of cancer cells was found to be through epigenetic demethylation of m^6A in the 3'UTR of BNIP3 (29). Also, the FTO-mediated tumor progression could be due to FTO involvement in EMT as was reported for breast cancer (28) and pancreas cancer (26). In the present study, we showed that FTO played an oncogenic role in HSCC and was involved in EMT. More specifically, we found that the expression of FTO in HSCC tissues was significantly elevated compared to normal tissues and was associated with a worse prognosis in patients with HSCC, whereas FTO knockdown in HSCC cells could

markedly inhibit proliferation, migration, and invasion *in vitro* and tumor growth and metastasis *in vivo*.

Previous studies showed that the oncogenic role of FTO in AML (22), glioblastoma (24), and cervical cancer (30), and its tumor-suppressor role in ovarian cancer (35) were specifically related to its catalytic demethylase properties. In line with these findings, we also found that, first, FTO contributed to an increase of global m^6A modification level in HSCC cells, and second, the enforced expression of the demethylase-inactive mutant FTO was unable to promote cell proliferation, migration, and invasion in FaDu cells.

FTO's influence on cancer development is intricately tied to its modulation of m^6A modifications within downstream genes (15). We identified SERPINE1 as a downstream target of FTO and specified the site within SERPINE1 mRNA sequence that was responsible for modulating SERPINE1 mRNA expression. SERPINE1 is encoded by plasminogen activator inhibitor type 1 (PAI-1), is an important inhibitor of tissue plasminogen activator and urokinase, and was found to take part in proliferation, metastasis, and therapeutic resistance in different malignancies (42-44). In HNSCC, SERPINE1 was previously found to promote cell proliferation and EMT (45) and its overexpression was associated with poor outcomes by promoting tumor aggressiveness and metastasis (46,47). In the present study, we found that, first, knockdown of SERPINE1 suppressed the malignant phenotypes of HSCC cells, second, its protein was involved in EMT progression, and third, the SERPINE1-silencing-associated inhibitory effects on EMT could be rescued through overexpression of FTO *in vitro*.

M^6A modification plays a vital role in the complexity of tumor microenvironment (TME) (48). Interaction between m6A modification and TME mediates the biological processes of cancer cells, immune cells, and stromal cells to influence tumor initiation, progression, and therapy responses. In recent years, compelling evidence have shown that dysfunction of multiple immune killer cells and abnormal secretion of immune-related factors can induce immunosuppression in the TME of HNSCC, and eventually led to the development of HNSCC (49,50). It has been suggested that ALKBH5/RIG-I/IFNα axis regulates immune microenvironment by m6A modification in HNSCC (51). In AML, FTO exerts a crucial influence on the self-renewal of tumor stem cells and immune evasion (52). SERPINE1, derived from cancer associated fibroblasts cells, enhanced the migratory and invasive capabilities of both ESCC cells and macrophages through the Akt and Erk1/2 signaling pathways (53). Therefore, in the subsequent phase of our study, we will explore whether FTO influences tumor progression in HSCC by modulating the immune microenvironment via the regulation of SERPINE1.

This study has confirmed the carcinogenic role of FTO in HNSCC. In 2019, Professor Jianjun Chen's team developed two new small molecule inhibitors of FTO, FB23 and FB23-2 (54), which directly bind FTO and specifically inhibit the m6A demethylase activity of FTO and inhibit the proliferation of acute myeloid leukemia cells, and are expected to be used in clinical research of the disease. Perhaps these inhibitors can be used as targeted therapies for hypopharyngeal squamous cell carcinoma in the future.

Conclusions

In conclusion, this study revealed that FTO played a critical oncogenic role in HSCC and the major functions of FTO were dependent on its catalytic activity. In addition, we identified SERPINE1 as a downstream target of FTO and demonstrated the direct influence of FTO on the m^6A methylation process of SERPINE1 mRNA. Our findings highlight the significance of FTO-mediated m^6A modification in promoting cancer progression and offer potential avenues for therapeutic interventions against HSCC through modulation of m^6A modification.

Acknowledgments

None.

Footnote

Reporting Checklist: The authors have completed the ARRIVE and MDAR reporting checklists. Available at https://tcr.amegroups.com/article/view/10.21037/tcr-2024-2507/rc

Data Sharing Statement: Available at https://tcr.amegroups.com/article/view/10.21037/tcr-2024-2507/dss

Peer Review File: Available at https://tcr.amegroups.com/article/view/10.21037/tcr-2024-2507/prf

Funding: This work was supported by the National Natural Science Foundation of China (No. 82172961) and the Major Science and Technology Plan Project of Hainan Province (No. ZDKJ202005).

Conflicts of Interest: All authors have completed the ICMJE uniform disclosure form (available at https://tcr.amegroups.com/article/view/10.21037/tcr-2024-2507/coif). The authors have no conflicts of interest to declare.

Ethical Statement: The authors are accountable for all aspects of the work in ensuring that questions related to the accuracy or integrity of any part of the work are appropriately investigated and resolved. The study was conducted in accordance with the Declaration of Helsinki (as revised in 2013). The study was approved by Ethical Committee of Shandong Provincial ENT Hospital (No. 20210243) and informed consent was taken from all the patients. Animal experiments were performed according to the Guide for the Care and Use of Laboratory Animals of the National Research Council (8th edition), and were approved by the Ethics Committee of Shandong Provincial ENT Hospital (No. 20210213).

References

1. Ferlay J, Colombet M, Soerjomataram I, et al. Cancer statistics for the year 2020: An overview. Int J Cancer 2021. [Epub ahead of print]. doi: 10.1002/ijc.33588.
2. Bray F, Laversanne M, Sung H, et al. Global cancer statistics 2022: GLOBOCAN estimates of incidence and mortality worldwide for 36 cancers in 185 countries. CA Cancer J Clin 2024;74:229-63.
3. Johnson DE, Burtness B, Leemans CR, et al. Head and neck squamous cell carcinoma. Nat Rev Dis Primers 2020;6:92.
4. Kwon DI, Miles BA; . Hypopharyngeal carcinoma: Do you know your guidelines? Head Neck 2019;41:569-76.
5. Cooper JS, Porter K, Mallin K, et al. National Cancer Database report on cancer of the head and neck: 10-year update. Head Neck 2009;31:748-58.
6. Newman JR, Connolly TM, Illing EA, et al. Survival trends in hypopharyngeal cancer: a population-based review. Laryngoscope 2015;125:624-9.
7. Ou X, Zhai R, Wei W, et al. Induction Toripalimab and Chemotherapy for Organ Preservation in Locally Advanced Laryngeal and Hypopharyngeal Cancer: A Single-Arm Phase II Clinical Trial. Clin Cancer Res 2024;30:344-55.
8. Caudell JJ, Gillison ML, Maghami E, et al. NCCN Guidelines® Insights: Head and Neck Cancers, Version 1.2022. J Natl Compr Canc Netw 2022;20:224-34.
9. Frye M, Harada BT, Behm M, et al. RNA modifications modulate gene expression during development. Science 2018;361:1346-9.
10. Zhao BS, Roundtree IA, He C. Post-transcriptional gene regulation by mRNA modifications. Nat Rev Mol Cell Biol 2017;18:31-42.
11. Dominissini D, Moshitch-Moshkovitz S, Schwartz S, et al. Topology of the human and mouse m6A RNA methylomes revealed by m6A-seq. Nature 2012;485:201-6.
12. Wang X, Zhao BS, Roundtree IA, et al. N(6)-methyladenosine Modulates Messenger RNA Translation Efficiency. Cell 2015;161:1388-99.
13. Meyer KD, Saletore Y, Zumbo P, et al. Comprehensive analysis of mRNA methylation reveals enrichment in 3' UTRs and near stop codons. Cell 2012;149:1635-46.
14. Meyer KD, Jaffrey SR. Rethinking m(6)A Readers, Writers, and Erasers. Annu Rev Cell Dev Biol 2017;33:319-42.
15. He L, Li J, Wang X, et al. The dual role of N6-methyladenosine modification of RNAs is involved in human cancers. J Cell Mol Med 2018;22:4630-9.
16. Zhang S, Zhao BS, Zhou A, et al. m(6)A Demethylase ALKBH5 Maintains Tumorigenicity of Glioblastoma Stem-like Cells by Sustaining FOXM1 Expression and Cell Proliferation Program. Cancer Cell 2017;31:591-606.e6.
17. Yue B, Song C, Yang L, et al. METTL3-mediated N6-methyladenosine modification is critical for epithelial-mesenchymal transition and metastasis of gastric cancer. Mol Cancer 2019;18:142.
18. Ma JZ, Yang F, Zhou CC, et al. METTL14 suppresses the metastatic potential of hepatocellular carcinoma by modulating N(6) -methyladenosine-dependent primary MicroRNA processing. Hepatology 2017;65:529-43.
19. Fawcett KA, Barroso I. The genetics of obesity: FTO leads the way. Trends Genet 2010;26:266-74.
20. Frayling TM, Timpson NJ, Weedon MN, et al. A common variant in the FTO gene is associated with body mass index and predisposes to childhood and adult obesity.

Science 2007;316:889-94.
21. Jia G, Fu Y, Zhao X, et al. N6-methyladenosine in nuclear RNA is a major substrate of the obesity-associated FTO. Nat Chem Biol 2011;7:885-7.
22. Li Z, Weng H, Su R, et al. FTO Plays an Oncogenic Role in Acute Myeloid Leukemia as a N(6)-Methyladenosine RNA Demethylase. Cancer Cell 2017;31:127-41.
23. Kou R, Li T, Fu C, et al. Exosome-shuttled FTO from BM-MSCs contributes to cancer malignancy and chemoresistance in acute myeloid leukemia by inducing m6A-demethylation: A nano-based investigation. Environ Res 2024;244:117783.
24. Cui Q, Shi H, Ye P, et al. m(6)A RNA Methylation Regulates the Self-Renewal and Tumorigenesis of Glioblastoma Stem Cells. Cell Rep 2017;18:2622-34.
25. Yang S, Wei J, Cui YH, et al. m(6)A mRNA demethylase FTO regulates melanoma tumorigenicity and response to anti-PD-1 blockade. Nat Commun 2019;10:2782.
26. Garg R, Melstrom L, Chen J, et al. Targeting FTO Suppresses Pancreatic Carcinogenesis via Regulating Stem Cell Maintenance and EMT Pathway. Cancers (Basel) 2022;14:5919.
27. Tang X, Liu S, Chen D, et al. The role of the fat mass and obesity-associated protein in the proliferation of pancreatic cancer cells. Oncol Lett 2019;17:2473-8.
28. Ou B, Liu Y, Gao Z, et al. Senescent neutrophils-derived exosomal piRNA-17560 promotes chemoresistance and EMT of breast cancer via FTO-mediated m6A demethylation. Cell Death Dis 2022;13:905.
29. Niu Y, Lin Z, Wan A, et al. RNA N6-methyladenosine demethylase FTO promotes breast tumor progression through inhibiting BNIP3. Mol Cancer 2019;18:46.
30. Zou D, Dong L, Li C, et al. The m(6)A eraser FTO facilitates proliferation and migration of human cervical cancer cells. Cancer Cell Int 2019;19:321.
31. Rong ZX, Li Z, He JJ, et al. Downregulation of Fat Mass and Obesity Associated (FTO) Promotes the Progression of Intrahepatic Cholangiocarcinoma. Front Oncol 2019;9:369.
32. Yang X, Shao F, Guo D, et al. WNT/β-catenin-suppressed FTO expression increases m(6)A of c-Myc mRNA to promote tumor cell glycolysis and tumorigenesis. Cell Death Dis 2021;12:462.
33. Wen L, Pan X, Yu Y, et al. Down-regulation of FTO promotes proliferation and migration, and protects bladder cancer cells from cisplatin-induced cytotoxicity. BMC Urol 2020;20:39.
34. Yi W, Yu Y, Li Y, et al. The tumor-suppressive effects of alpha-ketoglutarate-dependent dioxygenase FTO via N6-methyladenosine RNA methylation on bladder cancer patients. Bioengineered 2021;12:5323-33.
35. Huang H, Wang Y, Kandpal M, et al. FTO-Dependent N (6)-Methyladenosine Modifications Inhibit Ovarian Cancer Stem Cell Self-Renewal by Blocking cAMP Signaling. Cancer Res 2020;80:3200-14.
36. Ruan DY, Li T, Wang YN, et al. FTO downregulation mediated by hypoxia facilitates colorectal cancer metastasis. Oncogene 2021;40:5168-81.
37. Wang F, Liao Y, Zhang M, et al. N6-methyladenosine demethyltransferase FTO-mediated autophagy in malignant development of oral squamous cell carcinoma. Oncogene 2021;40:3885-98.
38. Li X, Chen W, Gao Y, et al. Fat mass and obesity-associated protein regulates arecoline-exposed oral cancer immune response through programmed cell death-ligand 1. Cancer Sci 2022;113:2962-73.
39. Jin S, Li M, Chang H, et al. The m6A demethylase ALKBH5 promotes tumor progression by inhibiting RIG-I expression and interferon alpha production through the IKKε/TBK1/IRF3 pathway in head and neck squamous cell carcinoma. Mol Cancer 2022;21:97.
40. Zhou Y, Zeng P, Li YH, et al. SRAMP: prediction of mammalian N6-methyladenosine (m6A) sites based on sequence-derived features. Nucleic Acids Res 2016;44:e91.
41. Zhang T, Berrocal JG, Frizzell KM, et al. Enzymes in the NAD+ salvage pathway regulate SIRT1 activity at target gene promoters. J Biol Chem 2009;284:20408-17.
42. Valiente M, Obenauf AC, Jin X, et al. Serpins promote cancer cell survival and vascular co-option in brain metastasis. Cell 2014;156:1002-16.
43. Giacoia EG, Miyake M, Lawton A, et al. PAI-1 leads to G1-phase cell-cycle progression through cyclin D3/cdk4/6 upregulation. Mol Cancer Res 2014;12:322-34.
44. Almholt K, Nielsen BS, Frandsen TL, et al. Metastasis of transgenic breast cancer in plasminogen activator inhibitor-1 gene-deficient mice. Oncogene 2003;22:4389-97.
45. Chen G, Sun J, Xie M, et al. PLAU Promotes Cell Proliferation and Epithelial-Mesenchymal Transition in Head and Neck Squamous Cell Carcinoma. Front Genet 2021;12:651882.
46. Pavón MA, Parreño M, Téllez-Gabriel M, et al. Gene expression signatures and molecular markers associated with clinical outcome in locally advanced head and neck carcinoma. Carcinogenesis 2012;33:1707-16.
47. Arroyo-Solera I, Pavón MÁ, León X, et al. Effect of serpinE1 overexpression on the primary tumor and lymph

node, and lung metastases in head and neck squamous cell carcinoma. Head Neck 2019;41:429-39.
48. Li Y, Su R, Deng X, et al. FTO in cancer: functions, molecular mechanisms, and therapeutic implications. Trends Cancer 2022;8:598-614.
49. Gavrielatou N, Doumas S, Economopoulou P, et al. Biomarkers for immunotherapy response in head and neck cancer. Cancer Treat Rev 2020;84:101977.
50. Greten FR, Grivennikov SI. Inflammation and Cancer: Triggers, Mechanisms, and Consequences. Immunity 2019;51:27-41.
51. Yang Z, Zhang S, Xiong J, et al. The m(6)A demethylases FTO and ALKBH5 aggravate the malignant progression of nasopharyngeal carcinoma by coregulating ARHGAP35. Cell Death Discov 2024;10:43.
52. Su R, Dong L, Li Y, et al. Targeting FTO Suppresses Cancer Stem Cell Maintenance and Immune Evasion. Cancer Cell 2020;38:79-96.e11.
53. Sakamoto H, Koma YI, Higashino N, et al. PAI-1 derived from cancer-associated fibroblasts in esophageal squamous cell carcinoma promotes the invasion of cancer cells and the migration of macrophages. Lab Invest 2021;101:353-68.
54. Huang Y, Su R, Sheng Y, et al. Small-Molecule Targeting of Oncogenic FTO Demethylase in Acute Myeloid Leukemia. Cancer Cell 2019;35:677-691.e10.

(English Language Editor: J. Gray)

Cite this article as: Sa N, Liu X, Hao D, Lv Z, Zhou S, Yang L, Jiang S, Tian J, Xu W. FTO-mediated m^{6}A demethylation of SERPINE1 mRNA promotes tumor progression in hypopharyngeal squamous cell carcinoma. Transl Cancer Res 2025;14(1):595-612. doi: 10.21037/tcr-2024-2507